J Mol Model (2011) 17:587–592
DOI 10.1007/s00894-010-0757-x

ORIGINAL PAPER

Molecular dynamics simulation of oseltamivir resistance in neuraminidase of avian influenza H5N1 virus

Mao Shu · Zhihua Lin · Yunru Zhang · Yuqian Wu · Hu Mei · Yongjun Jiang

Received: 3 January 2010 / Accepted: 12 May 2010 / Published online: 3 June 2010
© Springer-Verlag 2010

Abstract The outbreak of avian influenza virus H5N1 has raised a global concern because of its high virulence and mutation rate. Although two classes of antiviral drugs, M2 ion channel protein inhibitors and neuraminidase inhibitors, are expected to be important in controlling the early stages of a potential pandemic. Different strains of influenza viruses have differing degrees of resistance against the antivirals. In order to analyze the detailed information on the viral resistance, molecular dynamics simulations were carried out for the neuraminidase (NA) complex with oseltamivir. The carboxylate of Glu276 of H252Y NA faces toward the O-ethyl-propyl group of oesltamivir, Glu276 of wild-type NA adopts a conformation pointing away from the oesltamivir. $\tau 2$ and $\tau 3$ torsional angles fluctuation of the oesltamivir are relatively high for the H252Y mutant NA complex. In addition, there are fewer hydrogen bonds between the oesltamivir and H252Y mutation NA. The results show that H252Y mutation NA has high resistance against the drug.

M. Shu · Z. Lin · Y. Zhang
College of Pharmacy and Bioengineering,
Chongqing University of Technology,
Chongqing 400050, People's Republic of China

Y. Wu · H. Mei
College of Bioengineering, Chongqing University,
Chongqing 400030, People's Republic of China

Y. Jiang (✉)
Key Laboratory for Molecular Design and Nutrition Engineering of Ningbo City, Ningbo Institute of Technology,
Zhejiang University,
315100 Ningbo, Zhejiang Province, People's Republic of China
e-mail: yjjiang@nit.zju.edu.cn

Keywords Influenza virus · Molecular dynamics simulations · Neuraminidase · Oseltamivir

Introduction

The worldwide spread of the H5N1 avian influenza virus has caused several diseases in humans and raised serious concerns about a global flu pandemic [1]. Although vaccines are the primary line of defense for the prophylactic control of influenza virus infections, effective antiviral drugs provide are expected to be important in controlling the early stages of a potential pandemic. Surface membrane of influenza virus contains three important proteins: haemagglutinin, neuraminidase, and M2 protein. Haemagglutinin mediates cell-surface sialic acid receptor binding to initiate virus infection. Neuraminidase facilitates viral shedding by cleaving the sialic acid linkage formed between the HA and sialic receptors on the surface of the host cell. M2 protein regulates the internal pH of the virus, which is essential for uncoating of the virus during the early stages of viral replication [2]. Two classes of antiviral drugs can be used to treat influenza viruses: M2 ion channel protein inhibitors (amantadine and rimantadine), which act by hindering proton transfer through M2 channel, and neuraminidase inhibitors (oseltamivir and zanamivir), which interrupt influenza virus replication cycle by preventing release of the virus from infected cells and may interfere with its initial infection [3, 4]. Amantadine and rimantadine are limited application due to their adverse side effects [5–8]. Oseltamivir and zanamivir are safe and effective drugs for prophylaxis and early treatment of influenza virus infections in humans [9]. However, different strains of influenza viruses have differing degrees of resistance against oseltamivir [10–12]. These studies

describe mechanisms of resistance associated to the mutations neuraminidase, and their consequence in virus fitness and transmission [13]. It is required to understand the mechanism of oseltamivir resistance at the molecular level.

Molecular dynamics (MD) simulation is a useful theoretical tool to analyze the protein-ligand interactions with atomic resolution based on classical mechanics [14–16]. Previous MD simulations have been carried out on the drug-target interactions in the catalytic core domain of neuraminidase [17–20] and the novel druggable loop domain in the neuraminidase [21, 22]. These studies showed that important conformational interactions occur in the active region and open conformation of the loop residues region, but did not investigate neuraminidase mutation rendering the antiviral drug resistant fully.

The aim of this investigation is to disclose if there are significant differences in the dynamical behavior of the wild-type and mutant NA complex with oseltamivir based on the references which pointed that H252Y mutation neuraminidase has high resistance against the drug [23–25]. Here, we report MD investigation of interactions between oseltamivir and neuraminidase of H5N1 virus.

Methods

Preparation of the systems

The X-ray structure of neuraminidase subtype N1 complexed with oseltamivir (PDB code: 2HU4, H252Y mutant) was used as the initial structure of the mutant NA complexed [26]. The wild type NA structure was obtained from that mutated residue tyrosine(Y252) of H252Y mutant NA was changed to Histidine (H252). All missing hydrogen atoms of the proteins were added using the LEaP module in the AMBER 9 software package. All ionizable side chains of amino acid residues in the protein were configured in their characteristic ionization states at pH 7.0 using the LEaP module of AMBER. Oseltamivir was parameterized according to quantum chemical calculations, which included performing a geometry optimization with Gaussian98 [27] at the Hartree-Fock/6-31G* level. The resulting atomic charges were then determined according to the RESP method [28], and the atom types were assigned by the antechamber program [29]. Counterions were added to maintain the electroneutrality of all the systems. Each system was immersed in a 10 Å truncated octahedron periodic water box, and the structure water molecules were maintained. The box of water molecule in all cases contained around 8229 TIP3P [30] water molecules in each of the complex.

Molecular dynamics simulations

Molecular dynamics simulations were carried out on the two systems respectively using the SANDER module of AMBER 9.0 with the Amber FF03 [31, 32] and GAFF force field [33]. A 2 fs time step was used in all the simulations, and long-range electrostatic interactions were treated with the particle mesh Ewald (PME) procedure [34] with a 10 Å non-bonded cutoff. Bond lengths involving hydrogen atoms were constrained using the SHAKE algorithm [35]. All systems were minimized prior to the production run. The minimization, performed with the SANDER module under constant volume condition, consisted of 2 steps. First, the solvent molecules were relaxed, while all heavy atoms in both protein and oseltamivir were restrained with forces of 500 kcal mol^{-1} $Å^{-2}$. Then the whole systems were relaxed without any restraint. The 2 steps above involved 10,000 cycles of steepest descent followed by 5000 cycles of conjugate gradient minimization respectively. After the relaxation, 300 ps of MD simulations were carried out at constant volume, with 10 kcal mol^{-1} $Å^{-2}$ restraints on solute. Then the 10ns of NPT MD simulation were carried out on all systems at constant pressure of 1 atm. All simulations were performed at 300 K.

Results and discussion

Protein perturbative changes in the two models

To evaluate the stability of the simulated systems, RMSDs of wide-type and mutant complexes with inhibitor (all atoms) obtained during the 10-ns MD simulations relative to the initial structure. RMSD of the both systems are fairly stable around 2 Å, which indicated that the solvated systems are stable over the course of the simulation. A qualitative examination of the RMSD trajectories from these simulations systems suggest that both neuraminidase molecules might have undergone the similar conformation changing.

Comparing the superimposition of the two average structures were obtained from all simulations. Figure 1 indicates that the different conformational features observed in wild-type and mutant enzyme complexes.

The conformation of the active site residue Glu 276 marked rearrangement on drug binding to neuraminidases in the different complex [26], so we focused some attention on this residue. The carboxylate of Glu 276 makes bidenate interaction with the guanidinium group of Arg 224 on the both complexes, in the mutant NAcomplex, carboxylate of Glu 276 faces towards the O-ethyl-propyl group of oesltamivir and press the hydrophobic group of oseltamivir, it may destroy the interactions

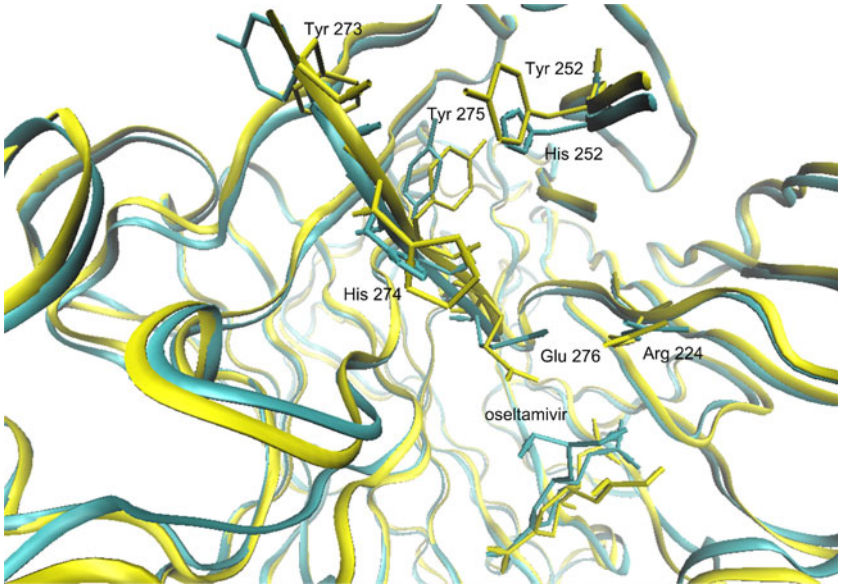

Fig. 1 Superposition of the wild-type (*green*) and H252Y mutant (*yellow*) neuraminidase average structures obtained from all simulations

between ammonium group of oseltamivir and active site residue Asp151 and presume that the H252Y mutant neuraminidase may resist to oseltamivir; by contrast, in wild-type complex, the carboxylate of Glu 276 adopts a conformation pointing away from O-ethyl-propyl group of oesltamivir, this makes more space for O-ethyl-propyl group of oesltamivir. By the further analyses, residue Tyr252 of H252Y mutant NA affects the conformation changing of the bulkier residue Tyr273 and Tyr275 by hydrogen bonds, and the conformation change of residue Tyr275 cause partially displacing for Glu 276; in wild-type NA, there is a smaller residue His at position 252, leaving space for His 274 to occupy without perturbing Glu 276. This is in agreement with reference [26].

Conformations of the inhibitor structure

It is well-known that small change to ligand structure can result in dramatically different binding orientation in the acceptor-ligand complex. The interaction between neuraminidase and oseltamivir in the two complexes as well as the influence of the inhibitor on the structural and dynamical properties of the active site region have been clarified by analyzing the trajectory data obtained from the MD simulations.

Figure 2 shows that the RMSDs of oseltamivr embedded in the neuraminidase pocket *vs*. simulation time. Interestingly, in wild-type NA complex, the RMSD of oseltamivir remains below ~1.5 Å during the whole simulation, and in H252Y mutant NA complex, it remains below ~2.0 Å during the first 4 ns, it reaches ~2.5 Å in following 1.5ns, afterward. And it descends back to ~2.0 Å again. The result reveals that oseltamivir is more flexible in H252Y mutant NA complex. To assess the structural flexibility of the oseltamivir, the torsional angles of their side chains were monitored. Five torsional angles, $\tau 1$–$\tau 5$, are described by sets of four heavy atoms as defined and indicated by arrows in Fig. 3. The plots were evaluated over the last 4ns of MD trajectories of the two systems studied and are compared in Fig. 4. $\tau 1$ torsional angle of both neuraminidase complexes is found at almost 5°. This may be that the carboxylate group (—COO-) was observed to lie parallel to the oseltamivir 's ring and form H-bonds with residue Arg292 of neuraminidase. In the wild-type system, the $\tau 2$ and $\tau 3$ torsional angle of inhibitor fluctuates around −140° and −110° respectively, and in the

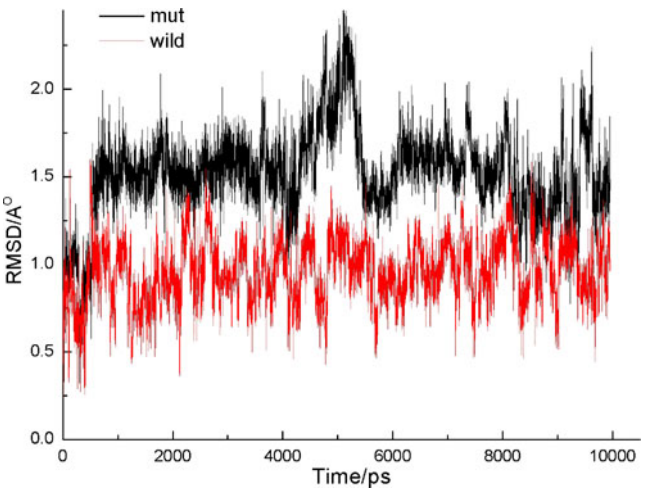

Fig. 2 RMSD of oseltamivir with respect to the equilibrated conformation as a function of time in the wild-type (*red*) and H252Y mutant(*black*) NA complexes

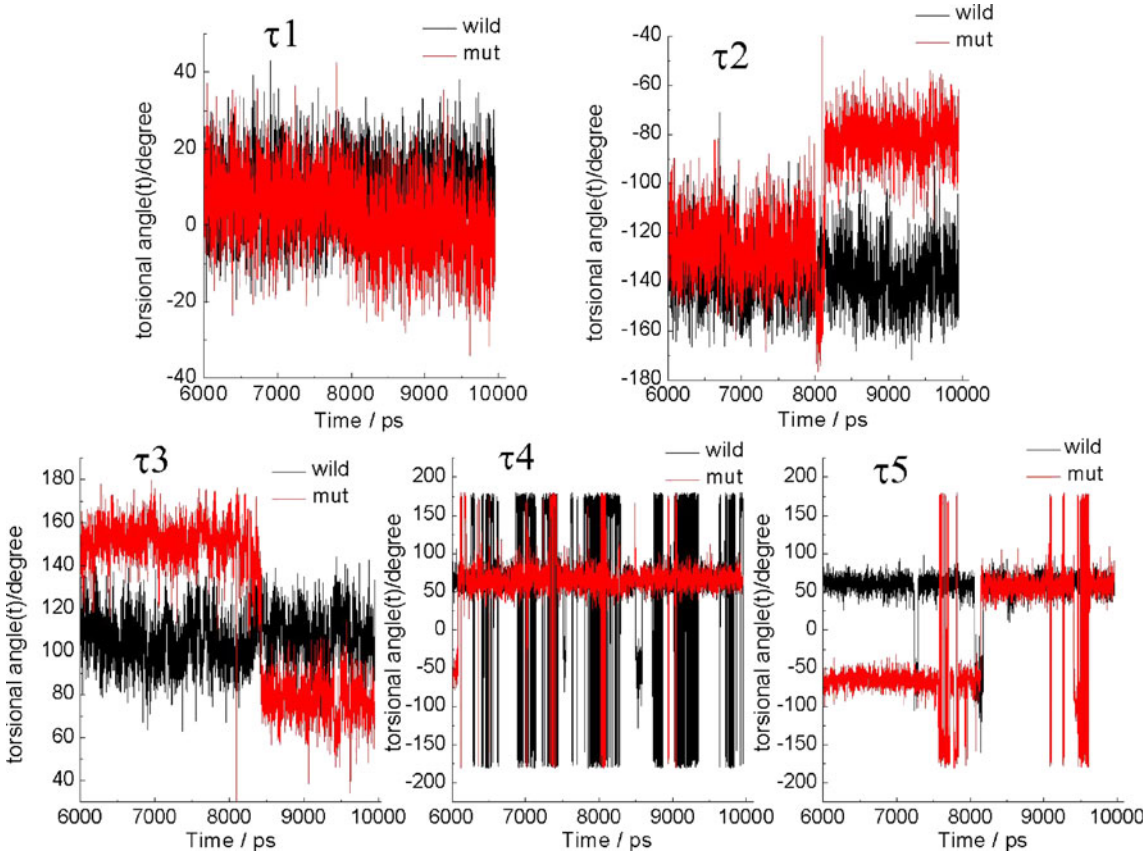

Fig. 3 Torsional angle for the oseltamivir inhibitor. τ1: C9-C2-C1-O1, τ2: C4-C5-N1-C6, τ3: C5-C8-O4-C10, τ4 :O4-C10-C12-C13, τ5: O4-C10-C11-C14

mutant system it shows the range from −70° to −130° and from 80° to 160° respectively. This may be due to more conformational change of active site residues in the H252Y mutant NA. The τ4 and τ5, the hydrophobic group, can rotate rather freely between −180°and 180° in the both complexes. By further analyses, the mutant residue Tyr252 changes the position and orientation of residue Glu276, which was proposed to determine the low susceptibility of the ligand in inhibiting the neuraminidase enzyme [12].

Hydrogen bonds in the inhibitor-enzyme complex

The time evolution of the hydrogen bonds from the inhibitor-enzyme complex provided an approach to evaluate the convergence of the dynamical properties of the system. To qualify an interaction as a hydrogen-bond, we have used the default geometric criterion as defined in the program: the donor-acceptor heavy atom distance had to be shorter than 3.5 Å, the maximum distance between a hydrogen atom donor and an acceptor of 2.5 Å, and the donor-hydrogen-acceptor angle had to be larger than 120°.

Figure 5 shows that a high number of strong hydrogen bonds (% occupation≥80) is measured between the carboxyl group (-COO-) of the oseltamivir and its nearest

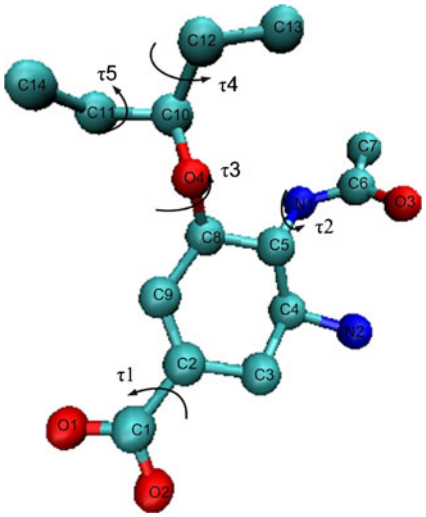

Fig. 4 Plots of oseltamivir torsional angles distribution sampleing over the last 4ns of MD simulation in the wild-type (*black*) and H252Y mutant (*red*) NA complexes

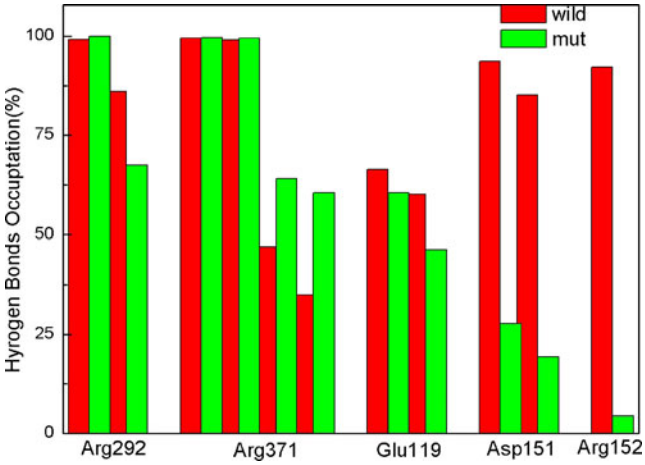

Fig. 5 Percent occupation pattern of hydrogen bonds between oseltamivir and binding pocket residues of the wild-type (*red*) and H252Y mutant (*blue*) NA

residues. About six hydrogen bonds with Arg292and Arg371 were formed for two complexes, this is consistent with previous reports [18]. The ammonium group of oseltamivir in the wild-type is stabilized by hydrogen bonding interactions with the two negatively charged residues Glu119 and Asp151. Referring to Masukawa et al. [17], hydrogen bonds with Asp151 were also found for the different neuraminidase complexes. Meanwhile, Glu119 makes hydrogen bond nets with residue Arg118 and the ammonium group of the oseltamivir, it should show that neuraminidase is more sensitive to oseltamivir in the wild-type complex. For amide group of oseltamivir, the inhibitor-enzyme interactions of the two complexes are comparable with hydrogen bonds with Arg152 residue, there is more higher hydrogen bonds occupations (92%) for the wild-type NA complex. This could be the reason why the amide side chain of oseltamivir in the wild-type system rotated only within a narrow range at the position around its preferential configuration (see $\tau 2$ in Fig. 4). Figure 6 shows that the hydrogen bonds between oseltamivir inhibitor and the pocket residues of wild-type (green) and H252Y mutant (yellow) neuraminidases. From Figs. 5 and 6, it can be seen that there are more hydrogen bonds between the oseltamivir and wild-type NA, and presume that H252Y mutant NA has high resistance against the oseltamtivir.

Conclusions

We have analyzed in detail the dynamic behavior of the wild-type and His252Tyr mutant NA complexes with the oseltamivir. Significant structural differences of protein was found at the catalytic residue Glu276, carboxylate of Glu 276 of H252Y NA faces toward the O-ethyl-propyl group of oesltamivir, by contrast, Glu 276 of wild-type NA adopts a conformation pointing away from the oesltamivir. Major structural differences of inhibitor were that the $\tau 2$ and $\tau 3$ torsional angle of inhibitor fluctuates range are small in the wild-type NA complex. In addition, there is higher hydrogen bond occupation (92%) in the wild-type NA complex. This work has provided insights into some detailed mechanism of action of the neuraminidase inhibitor and suggested the cause of neuraminidase inhibition and drug resistance. Based on these results, it will be useful for designing new antiviral drugs with high potency against both wild-type and drug-resistant strains of neuraminidase.

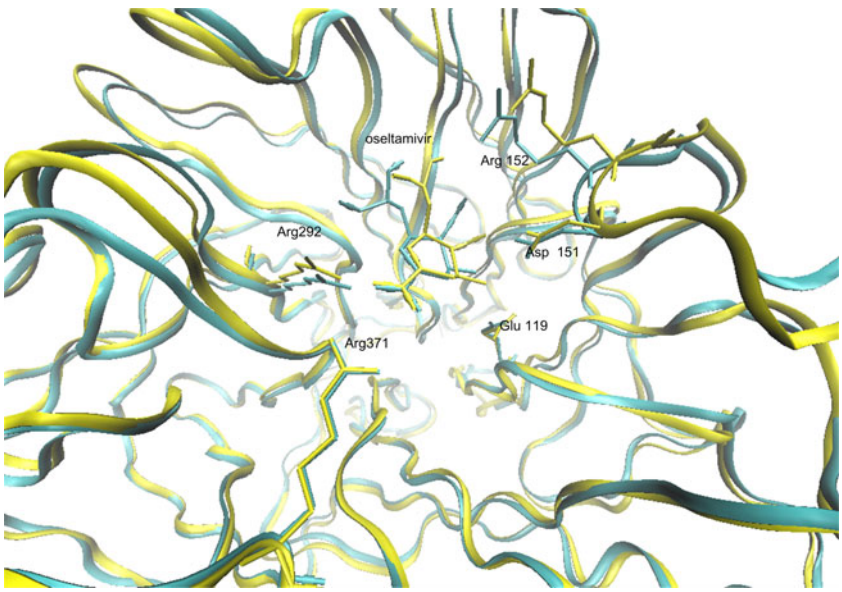

Fig. 6 The hydrogen bonds between oseltamivir and the binding pocket residues of wild-type (*green*) and H252Y mutant (*yellow*) NA

Acknowledgments This study was supported by the National Natural Science Foundation of China (No. 60873103), and supported by the Key Project of Natural Science Foundation of China (No. 30830090), and supported by Program for New Century Excellent Talents in University (No.NCET-06-0780), and supported by Visitorg Scholar Foundation of Key Laboratory of Biorheological Science and Technology (No. 2009BST03).

References

1. Enserink M (2005) Avian influenza: pandemic influenza: global update. Science 309:370–371
2. de Jong MD, Hien TT (2006) Avian influenza A (H5N1). J Clin Virol 35:2–13
3. Colman PM (1994) Influenza virus neuraminidase: structure, antibodies, and inhibitors. Protein Sci 3:1687–1696
4. Matrosovich MN, Matrosovich TY, Gray T et al (2004) Neuraminidase is important for the initiation of influenza virus infection in human airway epithelium. J Virol 78:12665–12667
5. Douglas RG Jr (1990) Prophylaxis and treatment of influenza. N Engl J Med 322:443–450
6. Wintermeyer SM, Nahata MC (1995) Rimantadine: a clinical perspective. Ann Pharmacother 29:299–310
7. Pinto LH, Holsinger LJ, Lamb RA (1992) Influenza virus M2 protein has ion channel activity. Cell 69:517–528
8. Hay AJ et al (1993) In: Hannoun CE (ed) Options for the control of influenza virus II. Excerpta Medica, Amsterdam, pp 281–288
9. Jefferson T, Demicheli V, Rivetti D et al (2006) Antivirals for influenza in healthy adults: systematic review. Lancet 367: 303–313
10. Gubareva LV, Kaiser L, Matrosovich MN et al (2001) Selection of influenza virus mutants in experimentally infected volunteers treated with oseltamivir. J Infect Dis 183:523–531
11. McKimm-Breschkin JL (2000) Resistance of influenza viruses to neuraminidase inhibitors—a review. Antiviral Res 47:1–17
12. Moscona A (2005) Oseltamivir resistance-disabling our influenza defenses. N Engl J Med 353:2633–2636
13. Ferraris O, Lina B (2008) Mutations of neuraminidase implicated in neuraminidase inhibitors resistance. J Clin Virol 41:13–19
14. Adcock SA, McCammon JA (2006) Molecular dynamics: survey of methods for simulating the activity of proteins. Chem Rev 106:1589–1615
15. van Gusteren WF, Bakowies D, Baron R et al (2006) Biomolecular modeling: goals, problems, perspectives. Angew Chem Int Ed Eng 45:4064–4092
16. Ravna AW, Sylte I, Dahl SG (2009) Structure and localisation of drug binding sites on neurotransmitter transporters. J Mol Model 15:1155–1164
17. Masukawa KM, Kollman PA, Kuntz ID (2003) Investigation of Neuraminidase Substrate Recognition Using Molecular Dynamics and Free Energy Calculations. J Med Chem 46: 5628–5637
18. Malaisree M, Rungrotmongkol T, Decha P et al (2008) Understanding of known drug-target interactions in the catalytic pocket of neuraminidase subtype N1. Proteins 17:1908–1918
19. Malaisree M, Rungrotmongkol T, Nunthaboot N et al (2009) Source of oseltamivir resistance in avian influenza H5N1 virus with the H274Y mutation. Amino Acids 37:725–732
20. Udommaneethanakit T, Rungrotmongkol T, Bren U et al (2009) Dynamic behavior of avian influenza a virus neuraminidase subtype H5N1 in complex with oseltamivir, zanamivir, peramivir, and their phosphonate analogues. J Chem Inf Model 49:2323–2332
21. Amaro RE, Minh DD, Cheng LS et al (2007) Remarkable loop flexibility in avian influenza N1 and its implications for antiviral drug design. J Am Chem Soc 129:7764–7765
22. Landon MR, Amaro RE, Baron R et al (2008) Novel druggable hot spots in avian influenza neuraminidase H5N1 revealed by computational solvent mapping of a reduced and representative receptor ensemble. Chem Biol Drug Des 71:106–116
23. Rameix-Welti MA, Agou F, Buchy P et al (2006) Natural variation can significantly alter the sensitivity of influenza A (H5N1) viruses to oseltamivir. Antimicrob Agents Chemother 50:3809–3815
24. Govorkova EA, Ilyushina NA, Boltz DA, Douglas A, Yilmaz N, Webster RG (2007) Efficacy of oseltamivir therapy in ferrets inoculated with different clades of H5N1 influenza virus. Antimicrob Agents Chemother 51:1414–1424
25. McKimm-Breschkin JL, Selleck PW, Usman TB et al (2007) Reduced sensitivity of influenza A (H5N1) to oseltamivir. Emerging Infectious Diseases 13:1354–1357
26. Russell RJ, Haire LF, Stevens DJ et al (2006) The structure of H5N1 avian influenza neuraminidase suggests new opportunities for drug design. Nature 443:45–49
27. Frisch MJ, Trucks GW, Schlegel HB et al (1998) Gaussian98, Revision A.7. Gaussian Inc, Pittsburgh, PA
28. Bayly C, Cieplak P, Cornell W et al (1993) A well-behaved electrostatic potential based method using charge restraints for deriving atomic charges—the RESP model. J Phys Chem 97:10269–10280
29. Wang J, Wang W, Kollman PA et al (2006) Automatic atom type and bond type perception in molecular mechanical calculations. J Mol Graph Model 25(2):247–260
30. Jorgensen WL, Chandrasekhar J, Madura J et al (1983) Comparison of simple potential functions for simulating liquid water. J Chem Phys 79:926–935
31. Duan Y, Wu C, Chowdhury S, Lee MC et al (2003) A point-charge force field for molecular mechanics simulations of proteins based on condensed-phase quantum mechanical calculations. J Comput Chem 24:1999–2012
32. Lee MC, Duan Y (2004) Distinguish protein decoys using a scoring function based on AMBER force field, short molecular dynamics simulations and the generalized born solvent model. Proteins 55(3):620–634
33. Wang J, Wolf RM, Caldwell JW et al (2004) Development and testing of a general Amber force field. J Comput Chem 25:1157–1174
34. Darden T, York D, Pedersen L (1993) Particle mesh Ewald—an Nlog(N) method for Ewald sums in large systems. J Chem Phy 98:10089–10092
35. Ryckaert JP, Ciccotti G, Berendsen HJC (1977) Numerical integration of the Cartesian equations of motion of a system with constraints: molecular dynamics of n-alkanes. J Comput Phys 23:327–341